OPTIMISING MATERIAL SELECTION FOR AIRCRAFT WING DESIGN USING RADAR MULTI-CRITERIA DECISION-MAKING AND SIMULATION APPROACHES

UDC:629.7:519.816:519.62
Original scientific paper https://doi.org/10.46793/adeletters.2025.4.4.5

Ilesanmi Daniyan[1,2*], Festus Fameso[3], Lanre Daniyan[4], Adefemi Adeodu[5], Humbulani Simon Phuluwa[2]

[1]Department of Mechatronics Engineering, Bells University of Technology, P.M.B. 1015, Ota, Nigeria
[2]Department of Industrial Engineering & Engineering management, University of South Africa, Florida, South Africa
[3]Centre for Climate Change, Water Security and Disaster Management, Department of Civil Engineering, Tshwane University of Technology, Pretoria, 0183, South Africa
[4]Department of Instrumentation, Centre for Basic Space Science, University of Nigeria, Nsukka, Nigeria
[5]Department of Project Management, Bells University of Technology, P.M.B. 1015, Ota, Nigeria

Abstract:
This study employs a multi-criteria decision-making (MCDM) support specifically the Ranking Based on Distance and Range (RADAR-DR) and Relative Assessment of Decision Alternatives with Ranges (RADAR-ABER) techniques for the selection of materials for the development of an aircraft wing. The ABAQUS® commercial software code was used for the modeling and simulation analyses to determine the suitability of selected materials such as aluminum, stainless steel, titanium alloy and carbon fibre for the load-bearing and lift-generation application of an aircraft wing. A static structural analysis was implemented to predict and analyse the structural response of the wing to aerodynamic loads. The results obtained from the RADAR techniques indicate that carbon fibre is the most suitable material for the intended application. Furthermore, the results obtained from the computer aided modeling and simulation indicated that carbon fibre outperformed other materials in terms of the strain and displacement response to the load stress. The simulation results show that the concentration of the maximum stress concentrations was experienced at the leading edge. The von Mises stress observed peaked at approximately 25 MPa at the leading edge and reduced to 7.0 MPa at the trailing edge; both were found to be significantly lower than the tensile strength material (3.20 GPa), thereby indicating sufficient structural integrity. These findings provide critical insights for sustainable aircraft design and materials development and can assist aircraft and materials developers in their quest for the sustainability of aircraft operation.

ARTICLE HISTORY
Received: 19 August 2025
Revised: 23 October 2025
Accepted: 3 December 2025
Published: 15 December 2025

KEYWORDS
Aircraft wing, Aluminum alloy
Carbon fibre, MCD, RADAR
Stainless steel, Sustainability
Reliability, Titanium alloy

1. INTRODUCTION

The aviation sector contributes 12% carbon dioxide (CO_2) emissions of 12% to the total emissions generated globally from the transportation sector, and aircraft accounts for 5% of CO_2 emitted into the environment [1]. To mitigate the CO_2 emissions from aircraft, there is a need to enhance their performance in terms of lightness, fuel efficiency, speed, and environmental sustainability by developing some materials for special applications in the aircraft system [1,2]. Lightweight aircraft are

*CONTACT: Ilesanmi Daniyan, e-mail: iadaniyan@bellsuniversity.edu.ng

often characterised by low energy consumption, which brings about a reduction in the carbon emission of greenhouse gases [1,2]. Furthermore, weight reduction usually results in enhanced acceleration, with an increased capacity in terms of travel cycle time [3]. Thus, high-performing materials coupled with effective component recovery into service at the end-of-life (EOL) is essential to achieve operational cost effectiveness, reduction in waste generation and environmental friendliness.

To promote energy efficiency and improve the environmental friendliness during all the phases of the product lifecycle, lightweight materials such as aluminum, titanium alloy, as well as composite are considered a potential replacement for steel-based materials [4].

In recent times, attention has been drawn to the use of polymer matrix composites such as carbon fibre for aerospace applications. This is due to their outstanding mechanical properties that have found significant applications in the transport sector, particularly in the development of aircraft components [5]. Carbon fibre is reported to be approximately 70% lighter than steel-based alloys and 40% lighter than aluminum alloys, thereby making it useful in aircraft applications where weight reduction is an important consideration [6-8]. By reducing the weight of an aircraft, the energy consumption will also reduce, thereby making its use both economical and environmentally friendly, with a tendency for a reduction in the carbon footprint. The high strength-to-weight ratio of carbon fibre promotes durability as well as a reduction in the weight of the aircraft and its energy consumption, thereby improving its fuel efficiency and aircraft performance. Carbon fibre is suitable for ideal for aircraft manufacturing because of its high strength-to-weight ratio, which is needed by the aircraft to overcome wind resistance, improve fuel efficiency, speed and environmental friendliness [5]. It is also corrosion-resistant [6], which makes the components developed from it durable, with a long lifespan of the aircraft components, coupled with chemical stability. This means that it can remain stable on a molecular level under different operating and environmental conditions, including air, heat, air, water, and pressure, amongst others. It can also withstand harsh or extreme environmental conditions. For greater durability, carbon fibre can be developed with additives such as Ultra Violet (UV) protection. Furthermore, carbon fibre is moisture resistant, which makes it suitable for the operation of aircraft in wet or humid climates and has high fatigue life [6,7] as well as low thermal expansion, thus making it a good insulator [5]. Although carbon fibre has some limitations for aerospace applications, such as the cost and processing methods. Carbon fibre is costly compared to the conventional materials used in aircraft manufacturing, coupled with the fact that it might be difficult to recycle at the end of its useful life. Thus, with the potential of carbon fiber, it is considered a suitable material for replacing some traditional materials used in aircraft manufacturing in aerospace applications. However, the use of light materials can also promote improvement in an aircraft's performance via reduction in drag and enhance fuel efficiency, thereby reducing the fuel costs. This also makes it a potential candidate for the development of some primary and secondary structures in aircraft [8]. Existing studies indicate that carbon fiber reinforced polymer (CFRP) composites can significantly reduce the weight of some aircraft components, such as the airframe, thereby reducing the fuel consumption and carbon emissions by at least 14 to 15% [9,10].

The processing of carbon fibre at elevated temperatures above 1000^{o}C may result in the generation of 20 tons of CO_2 to produce 1 ton of carbon fibre [11]. Its use for automobile parts may result in a 30% reduction in weight and a 50 ton reduction in CO_2 generated per 1 ton of carbon fibre over a life cycle of 10 years [12]. Furthermore, the aircraft's fuselage can be made lighter by 20% using carbon fibre, thereby resulting in a reduction of 1400 tons of CO_2 in the long run [12]. Furthermore, the aircraft's fuselage can be made lighter by 20% using carbon fibre, thereby resulting in a reduction of 1400 tons of CO_2 in the long run [12]. The demand and usage of carbon fibre due to its outstanding performance in the aerospace industry, contribute to the growth of the aviation carbon fibre market which increased from 1.5 billion USD in 2021 to 1.76 billion USD in 2022 and projected to increase to 2.67 billion USD by 2028 and 4.4 billion USD in 2031 with a compound annual growth rate (CAGR) of 7.51% and 11.4% respectively [9,10]. The aviation sector is gradually embracing the use of carbon fibre for component development due to the need for the development of low-weight, fuel-efficient aircraft components that will reduce emissions and cost of operation. It finds application in the development of a variety of aircraft components, such as the wings, fuselages, and engine cowlings [13]. Some aircraft manufacturers have started using carbon fibre. For instance, Boeing uses approximately 32-35 tons of carbon fiber in each of its 787 jets [9,10,13].

The aim of this study is to employ the combination of multi-criteria decision approaches,

namely the Ranking Based on Distance and Range (RADAR-DR) and Relative Assessment of Decision Alternatives with Ranges (RADAR-ABER), as well as computer aided modeling and simulation approach for the selection of the most suitable materials for the development of an aircraft wing.

The motivation for this study stems from the need to ensure aircraft sustainability and optimal performance via the selection of the right material for its wing development. The RADAR approach provides a decision support tool for material selection, while the modeling and simulation validate the mechanical behavior to ensure structural performance and safety. The combination of the RADAR techniques and simulation approach ensures the selection of a top-ranked material that meets the safety, performance and sustainability requirements of aircraft wing application.

The RADAR techniques can assist as a decision support in the selection of the most suitable material by evaluating several criteria simultaneously, such as strength-to-weight ratio, cost, and durability, among others. On the other hand, computational modelling and simulation have proven to be an effective technique for estimating critical structural parameters and responses of components such as aircraft wings during operation [14-16]. By simulating the wing's behaviour under various loading conditions, its response to loads, stresses, including the resulting deformation, and potential failure points under can be determined, thereby leading to safer and more efficient aircraft designs. Through static structural analysis, the structural response of the wing to aerodynamic loads can be determined.

Hence, the RADAR techniques act as a decision support for material selection, while the simulation method accounts for the materials' behaviours such as strain and deformation under the required loading conditions. Compared to existing studies that have used the RADAR MCDM and simulation method in isolation, this study contributes a hybrid MCDM-simulation method that leverages the strengths of ranking and decision-making approaches, as well as numerical validation via simulation. The proposed method can overcome the limitations of each of the methods by ranking materials and validating their behaviours for the intended application.

This study provides a robust platform for determining the magnitude of critical parameters such as stress and corresponding strain induced, as well as displacement, to determine the possible operational limits of the aircraft wing component.

2. MATERIALS AND METHODS

2.1 Development of Carbon Fibre for Aerospace Applications

The framework for the selection and development of materials for aircraft applications is shown in Fig. 1.

The selected materials find application in the development of aerospace components such as fuselage, wings and interior cabin. However, the focus of this study is the selection of the most suitable material for the development of an aircraft wing. The aircraft's wing is one of the critical components of the aircraft due to the fact that it primarily creates the aerodynamic lift required to overcome the aircraft's weight [17]. An aircraft's wings are geometrically defined in terms of their span, planform, twist or pitch angle distribution, and cross-section.

One of the major requirements for the design of the shape of an aircraft wing is high aerodynamic efficiency in reducing the drag and generating lift.
The materials considered in this research were: carbon fibre, aluminum alloy, titanium alloy and stainless steel.

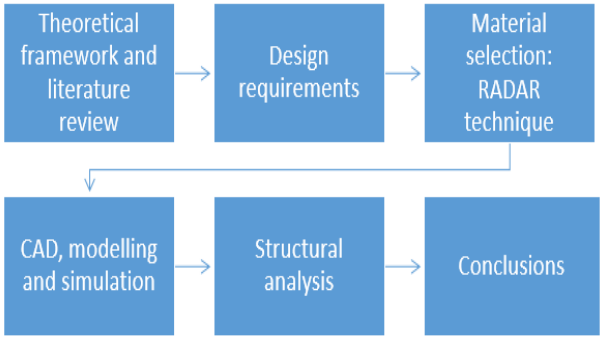

Fig. 1. The framework for the material selection for aircraft wing development

2.2 Multi-Criteria Decision-Making Techniques

This study employs the Ranking Based on Distance and Range Method (RADAR-DR) as well as the Relative Assessment of Decision Alternatives with Ranges-Alpha, Beta, Empty and Relative Relationship (RADAR-ABER) for the material selection for aircraft wing development. Trung et al. [11,18] stated that MCDMs are used as decision support for the selection of the most suitable alternative from conflicting multiple criteria, and have been widely deployed for ranking alternatives and as a decision support. However, their suitability depends on the applications [11,18].

2.2.1 Ranking Based on Distance and Range Method-Distance and Range (RADAR-DR)

This method was employed to objectively determine the ranking of alternatives (in this case, materials). It is an MCDM based on distance and range suitable for ranking alternatives. It determines the distance measures between each alternative and the ideal alternative in order to identify the best. It is simple and intuitive and can handle multiple criteria in a systematic manner. Furthermore, it scales data to ensure a fair comparison of the alternatives and to minimise bias [19,20].

The RADAR-DR method was implemented in this study by following the guidelines highlighted by Komatina [19,20]. The procedural steps include the following:

1. Construction of the decision matrix. This involves the listing of the alternatives as $A_1, A_2 \ldots . A_n$ where *n* is the number of alternatives (4). The alternatives in a serial order are carbon fibre, aluminum alloy, titanium alloy and stainless steel. The criteria are also listed as $C_1, C_2 \ldots . C_m$ where m is the number of criteria (4). The alternatives in a serial order are high strength to weight ratio, high strength at elevated temperatures, thermal insulation, high corrosion resistance with good impact resistance, and durability.
2. Normalisation of the decision matrix using the range method. For benefit criteria, each criterion j and alternative i, Eq. 1 holds thus:

$$x_{ij}^{/} = \frac{x_{ij} - min\,(x_j)}{\max(x_j) - min\,(x_j)} \quad (1)$$

   Where $x_{ij}^{/}$ is the normalised value, x_{ij} is the denotes the performace of alternative i on criterion j and x_j represents the set of values of all the alternatives under criterion j.
3. Definition of the ideal alternative. For the selection of the most suitable material, benefit criteria is employed, which takes 1 (max). It is assumed that the criteria have different levels of importance such that the weighted normalised matrix z_{ij} is expressed as Eq. 2a:

$$z_{ij} = w_j . x_{ij}^{/} \quad (2a)$$

where w_j are the weights assigned to the different criteria.

Hence, the ideal alternative is expressed as Eq. 2b while the worst performance is expressed as Eq. 2c.

$$z_{ij}{}^{*} = \max z_{ij} \quad (2b)$$

$$z_{ij}{}^{-} = \min z_{ij} \quad (2c)$$

4. Calculation of the Euclidean distance from the ideal alternative. Typically, the shortest distance to the ideal alternative ($D_i{}^{*}$) s usually the preferred alternative (Eq. 3a) while the distance from the worst alternative ($D_i{}^{-}$) is expressed as Eq. 3b.

$$D_i{}^{*} = \sqrt{\sum_{j=1}^{4}(z_{ij} - z_{ij}{}^{*})^2} \quad (3a)$$

$$D_i{}^{-} = \sqrt{\sum_{j=1}^{4}(z_{ij} - z_{ij}{}^{-})^2} \quad (3b)$$

5. Ranking of the alternatives. The alternatives are sorted out in ascending order and the smallest distance is ranked higher and selected as the preferred alternative. The RADAR score (C_i) of alternative i is computed from Eq. 4.

$$\mathrm{C}_i = \frac{D_i{}^{-}}{D_i{}^{-} + D_i{}^{*}} \quad (4)$$

Both RADAR methods employ numerical datasets allocated subjectively based on the author's understanding of the material properties from the insights gathered from the literature.

Table 1 presents the decision matrix featuring the allocation of a score (from 0-100) to the criteria based on their perceived importance.

The criteria, as displayed in Table 1, include a high strength-to-weight ratio to ensure that the selected material is light to promote energy efficiency and aerodynamic performance. For the second and third criteria, the material must demonstrate thermal insulation capability to ensure its suitability for high temperature application, while the last criterion stipulates that the material must be durable via effective resistance to corrosion and impact. The identification of these criteria was informed by synthesising some literature on material requirements for aircraft applications [1-3,15,16].

Table 1. The decision matrix for scores allocation to the criteria

Material	C1: Strength to weight	C2: Thermal insulation	C3: Strength at elevated temperature	C4: Corrosion and impact resistance
A1: Carbon fibre	95	85	85	70
A2: Aluminum alloy	80	60	60	60
A3: Titanium alloy	70	50	50	80
A4: Stainless steel	50	40	40	75

Eq. 1 was used for the normalisation of scores for each criterion.

For instance, for criterion C1 (max=95 and min=50).

$$A_1 = \frac{95-50}{95-50} = 1.00$$

$$A_2 = \frac{80-50}{95-50} = 0.67$$

$$A_3 = \frac{70-50}{95-50} = 0.44$$

$$A_4 = \frac{50-50}{95-50} = 0.00$$

The same calculation procedure was repeated for criterion C2 (max=85 and min=40), criterion C3 (max=80 and min=60) and criterion C4 (max=80 and min=60) to obtain the normalised matrix values displayed in Table 2.

Table 2. The normalised matrix for the alternatives and criteria

Material	C1 (strength to weight)	C2 (Thermal insulation	C3 (Strength at elevated temperature	C4 (Corrosion and impact resistance
A1: Carbon fibre	1.00	1.00	1.00	0.50
A2: Aluminum alloy	0.67	0.44	0.44	0.00
A3: Titanium alloy	0.44	0.22	0.22	1.00
A4: Stainless steel	0.00	0.00	0.00	0.75

2.2.2 Relative Assessment of Decision Alternatives with Ranges-Alpha, Beta, Empty and Relative Relationship (RADAR-ABER)

It is a MCDM that evaluates and rank alternatives when there are multiple and conflicting criteria by introducing four major matrices namely the alpha, beta, empty range ad relative relationship matrices to capture the performance range of the alternatives vis-à-vis the criterion. The decision matrix is constructed according to Table 3, comprising of alternative i on criterion j.

Thus $i = 1, 2 \ldots \ldots m$, and $j = 1, 2 \ldots \ldots \mathrm{n}$

Where m and n are the number of alternatives and criteria respectively. The second step is to normalise the weight for the benefit according to Eq. 1.

Table 3. The decision matrix

w	1	1	1	1
	j=1	j=2	j=3	j=4
i=1	95	85	85	70
i=2	80	60	60	60
i=3	70	50	50	80
i=4	50	40	40	75

The third step is to construct the alpha ($\propto_j$) and beta (β_j) scores using Eqs. 5 and 6, respectively. The computed α and β scores are presented in Tables 4 and 5 respectively. The α-scores represent the best scores for criterion j while β scores represent the worst scores for criterion j.

$$\propto_j = \max(x_{ij}^{/})\forall_j \quad (5)$$

$$\beta_j = \min(x_{ij}^{/})\forall_j \quad (6)$$

Where $\forall_j$ represents the effectiveness of criterion j.

Table 4. The α matrix

α matrix				
	j=1	j=2	j=3	j=4
i=1	0.345	0.320	0.320	0.495
i=2	0.426	0.486	0.486	0.571
i=3	0.492	0.576	0.576	0.429
i=4	0.655	0.680	0.680	0.460

Table 5. The β matrix

β matrix				
	j=1	j=2	j=3	j=4
i=1	0.655	0.680	0.680	0.505
i=2	0.574	0.514	0.514	0.429
i=3	0.508	0.424	0.424	0.571
i=4	0.345	0.320	0.320	0.540

The empty range score (Er_j) matrix is costructed according to Eq. 7 and the scores are presented in Table 6.

Small values of Er_j implies that the criterion could effectively separate the alternatives and vice versa:

$$\mathrm{Er}_j = 1 - (\alpha - \beta) \quad (7)$$

The relative relationship (rr_{jk}) matrix is constructed according to Eq. 8 which compares the criteria pairwise to establish their relationship importance and the contribution of one criterion over the other.

$$rr_{jk} = \frac{\alpha_j - \beta_j}{\alpha_k - \beta_k} \quad (8)$$

Where α_k and β_k represent the number of criteria for which an alternative is considered better and the number of criteria for which an alternative is considered worse respectively.

This is followed by the computation of the overall scores s_i by aggregating normalised performance h_{ij} with the derived weights $w_j$as expressed in Eq. 9 and the ranking of the alternatives according to their scores, where the alternative with the highest is the most preferred.

$$s_i = \sum_{j=1}^{n} w_j . h_{ij} \quad (9)$$

The scores are displayed in Table 7.

Table 6. The empty range matrix

Empty range matrix				
	j=1	j=2	j=3	j=4
i=1	0.310	0.360	0.360	0.010
i=2	0.148	0.029	0.029	0.143
i=3	0.016	0.153	0.153	0.143
i=4	0.310	0.360	0.360	0.079

Table 7. The Relative Relationship matrix

Relative relationship matrix				
	j=1	j=2	j=3	j=4
i=1	0.357	0.308	0.308	0.960
i=2	0.590	0.895	0.895	1.000
i=3	0.941	1.000	1.000	0.600
i=4	1.000	1.000	1.000	0.744

2.3 Computer-Aided Modelling and Simulation

Employing computer-aided modelling and simulation was essential to the nature of the comparative analysis that this study set out to achieve. Splichal et al. [21] indicate the feasibility of using the finite element analysis approach for determining the performance of materials such as composites for aircraft wings, focusing on the buckling behavior under dynamic loading. Computational modelling has proven to be an effective technique for estimating critical structural parameters and responses of components such as aircraft wings during operation. The ABAQUS® commercial software code (2022) was used for the predictive analysis of the suitability of the selected materials for the load-bearing and lift-generation application of an aircraft wing. Compared to other modelling and simulation tools, it provides a robust platform for linear and non-linear, implicit and explicit capabilities, multipysics support and advanced material modelling [22], thus, suitable for investigating the behaviour of materials intended for aircraft wing application and for establishing the feasible ranges of process parameters that determine the possible operational limits of the aircraft component. A static structural analysis was implemented to predict and analyse the structural response of the wing to aerodynamic loads. A Computer Aided Design (CAD) geometric model of the wing structure, as shown in Fig. 2, was created using the part drafting tool of the Complete ABAQUS environment (CAE).

2.3.1 Data Type and Source and Type for the Computer-Aided Modelling and Simulation

The data employed for the computer aided modeling and simulation include the geometric data (which encompasses the aircraft wing dimensions illustrated in Fig. 2), the various materials properties, the loading, boundary conditions and simulation data (imported from the standard library of the ABAQUS software).

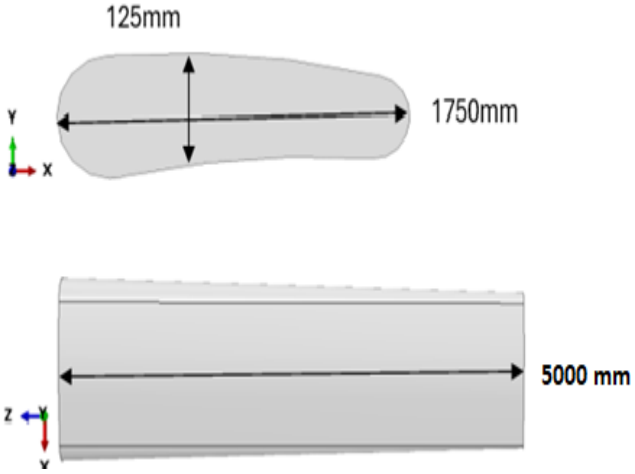

Fig. 2. An illustration of the aircraft wing

2.3.2 Meshing and Finite Element Analysis of the Aircraft's Wing Model

The geometry was meshed into finite analysis domains with 8-node three-dimensional hexahedral brick elements, allowing the simulation to evaluate feasible ranges of process parameters. The setup imposed encastre mechanical boundary conditions at the major chord end of the wing to simulate the real-life attachment of an aircraft wing to the fuselage machining, with specified mechanical interactions to define the wing's translational and rotational degrees of freedom.

The loads employed in this study represent the typical loads usually imposed on a typical large aircraft wing during flight [17].

The assembly was subjected to convergence simulations with mesh refinement for optimal accuracy and computational efficiency. An average global mesh size of 0.5 mm was adopted in order to balance computational cost and accuracy. Atmospheric pressure and lift force similar in magnitude and line of action to 'as is' conditions were applied respectively to the leading edge and base of the part as shown in Fig. 3. The component was subsequently configured to run for analysis under a static general stress analysis step under the same loading conditions but with different structural materials to assess their performance, with the loads applied to simulate the real-world operating conditions of the aircraft. Overall, these simulations provided valuable insights into the behaviour of components under different structural conditions, informing design and material selection decisions, especially concerning the structural reliability and stability of the wing.

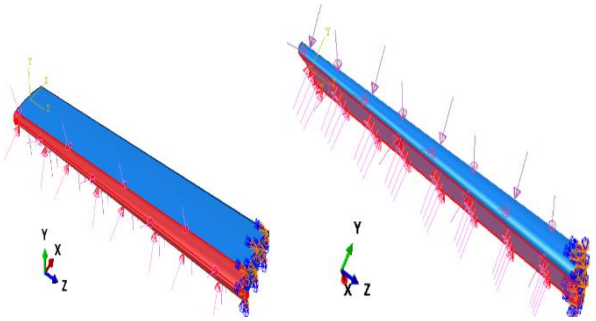

(a) (b)

Fig. 3. (a) Atmospheric pressure force, (b) Lift force applied to the geometric model of the wing.

Fig. 4 shows the linear hexahedral element of type C3D8R employed, having a total number of nodes of 39597 and elements of 31200.

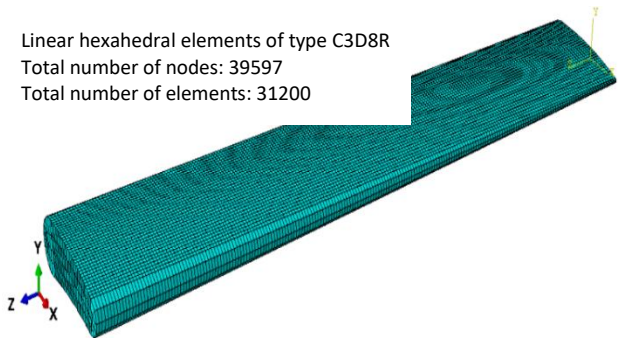

(a)

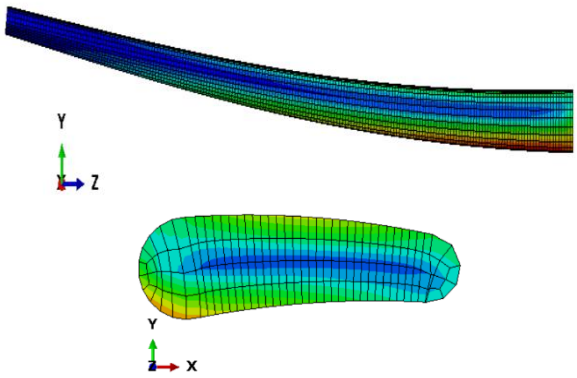

(b)

Fig. 4. (a) Linear hexahedral element of type C3D8R, (b) The meshed elements

The geometrical parameters that determine wing's shape include the span, chord distribution, aspect ratio, wing area, Planform area, winglets, etc. [17]. The selection of the right values of parameters will help reduce the overall wing drag. The major design requirement is to have an optimum lift-to-drag ratio so that the wing can be propelled for effective aerodynamic lift. There is a need to achieve a balance in the structural design of the wing in terms of its strength and stiffness and its aerodynamic capacity. The use of winglets can lead to significant reductions in drag, thereby promoting energy efficiency [17]. Thus, the wing is an essential component of the aircraft that determines the characteristics of the flight.

The planform area of the wing (S), is expressed as Eq. 4.

$$S = \int_{-s}^{s} c dy = \int_{-b/2}^{b/2} c dy \quad (4)$$

Since both wings are designed to have the same geometry then, Eq. 5 holds thus;

$$S = 2\int_{0}^{s} c dy = 2\int_{0}^{b/2} c dy \quad (5)$$

The aspect ratio (AR) is expressed as Eq. 6.

$$AR = \frac{b^2}{S} = \frac{4s^2}{S} = \frac{4s^2}{2\int_0^s c dy} \quad (6)$$

Where s - is the wing's semi-span designed as 5,000 mm (5 m) as shown in Fig. 2, b - is the wingspan (mm), c - is the local chord length (mm) and dy - represents the small increment along the half-span.

Leishman [17] stated that the typical values of aspect ratio ranges as follows:

1. Small general aviation aircraft: between 5 and 10.
2. Commercial transport aircraft: between 9 and 15.
3. Glider or sailplane: 30 and above.

This wing, designed in this study, is tailored towards a commercial transport aircraft; therefore, an average aspect ratio (AR) of 12 is selected.

From Eq. 4, the planform area (S) is calculated as 8.33 m^2 (corrected to 10 m^2 using a safety factor of 1.2), while the wing span *b* is calculated as 10.95 m.

3. RESULTS AND DISCUSSION

3.1 Result obtained for the Ranking Based on Distance and Range Method (RADAR-DR)

Taking the benefit criteria as $X^* = [1, 1, 1, 1]$ from Eq. 3a, the Euclidean distances of the alternatives from the ideal alternative were calculated as follows:

$$D_1^* = \sqrt{(1-1)^2 + (1-1)^2 + (0.5-1)^2 + (1-1)^2} = 0.50$$
$$D_2^* = \sqrt{(0.67-1)^2 + (0.44-1)^2 + (0-1)^2 + (0.5-1)^2} = 1.30$$
$$D_3^* = \sqrt{(0.44-1)^2 + (0.22-1)^2 + (1-1)^2 + (0.75-1)^2} = 0.99$$
$$D_4^* = \sqrt{(0-1)^2 + (0-1)^2 + (0.75-1)^2 + (0-1)^2} = 1.75$$

Table 8 presents the ranking of the materials in ascending order. The alternative with the shortest distance to the ideal alternative, as determined from the calculated Euclidean distances, represents the most suitable option based on the identified criteria.

Table 8. Ranking of the materials using the RADAR-DR method

Alternatives (Materials)	Euclidean distance (D_i)	Rank
A1: Carbon fibre	0.50	1
A2: Titanium alloy	0.99	2
A3: Aluminum alloy	1.30	3
A4: Stainless steel	1.75	4

The ranking done using the RADAR-DR techniques, ranked carbon fibre as the most suitable material for the development of the aircraft wing and ranked stainless steel least.

3.2 Relative Assessment of Decision Alternatives with Ranges-Alpha, Beta, Empty and Relative Relationship (RADAR-ABER)

Table 9 displays the ranking of the materials using the RADAR- ABER method. The order of the ranked alternatives agrees perfectly with the ranking order obtained using the RADAR-DR. This implies that the methods can be used as MCDM for material selection.

Table 9. Ranking of the materials using the RADAR- ABER method

i	Ranking index			Rank
	Alternatives	Sum	RI	
i=1	Carbon fibre	1.933	1.000	1
i=2	Titanium alloy	3.380	0.572	2
i=3	Aluminum alloy	3.541	0.546	3
i=4	Stainless steel	3.744	0.516	4

3.3 Results obtained from the Modeling and Simulation Technique

In Figs. 5-16, the horizontal axes are the true distances along the path (in mm), which represent the length along the wing, while the vertical axes represent the amount of stress, strain and deflection or deformation experienced by the materials for the stress, strain and displacement plots, respectively.

Fig. 5 shows the stress induced in the tested materials at the leading and trailing edges, respectively. The leading edge is the front part of the aircraft's wing that contacts the air, while the trailing edge is the rear part of the wing. The results indicated that by approximation, the magnitude of stress induced in the tested materials was the same (about 25 MPa at the leading-edge and 7.0 MPa at the trailing edge). The stresses induced decrease with an increase in the true distance along the path for all the materials.

Fig. 6 shows the maximum strain (E_{max}) of the materials along the leading and trailing edges of the aircraft. The results obtained indicated that the strain induced in the aluminum material is the highest, exceeding 0.35 and 80 for the leading and trailing edges respectively. This is followed by a titanium alloy whose strain values exceed 0.20 for the leading edge and 45 for the trailing edge. The lowest strain was observed in carbon fibre, whose strain values slightly exceeded 0.10 for the leading edge and 20 for the trailing edge, followed by stainless steel, whose strain values slightly exceeded 0.12 for the leading edge and 25 for the trailing edge. The maximum strain was observed to decrease with an increase in the true distance along the path for all the materials.

Fig. 7 shows that there was negligible Equivalent Plastic Strain (PEEQ) for the tested materials, while Fig. 8 shows the resultant displacement (U_{mag}) of the materials. The resultant displacement was highest in

aluminum (about 0.60 mm), followed by titanium alloy (0.30 mm) for both the leading and trailing edges. The resultant displacement was observed to increase with an increase in the true distance along the path for all the materials.

Carbon fibre has the lowest displacement (about 0.09 mm), followed by stainless steel (about 0.11 mm). Figs. 9 and 10 present the backward displacement (U1) and the upward displacement (U2) for the leading and trailing edges. The backward displacement was highest in aluminum (exceeding 0.020 mm), followed by titanium alloy (approximately 0.0125 mm). Carbon fibre has the lowest displacement (about 0.005 mm), followed by stainless steel (about 0.07 mm). The upward displacement was highest in aluminum (exceeding 0.60 mm), followed by titanium alloy (approximately 0.35 mm). Carbon fibre has the lowest displacement (about 0.12 mm), followed by stainless steel (about 0.15 mm). The magnitude of the upward and backward displacements was observed to increase with an increase in the true distance along the path for all the materials.

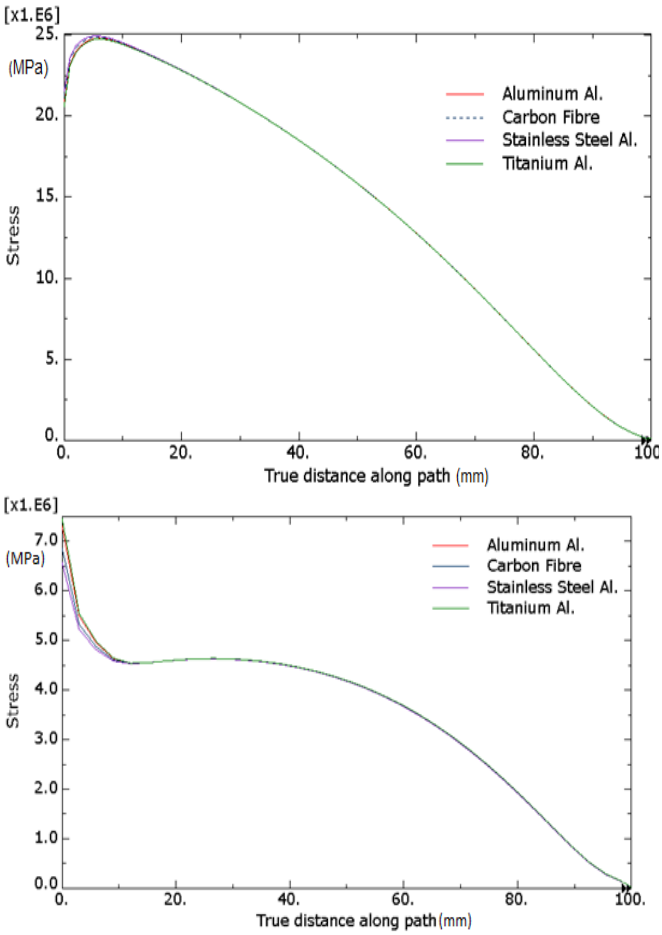

Fig. 5. Stress of the tested materials at the leading and trailing edges

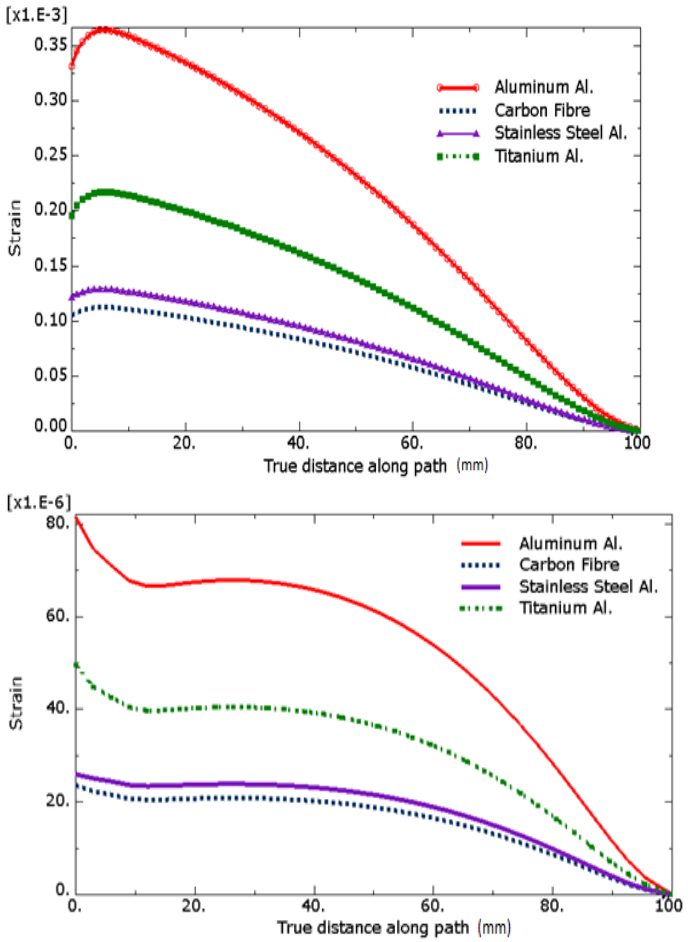

Fig. 6. Maximum Strain (Emax) of the materials along the leading and trailing edges

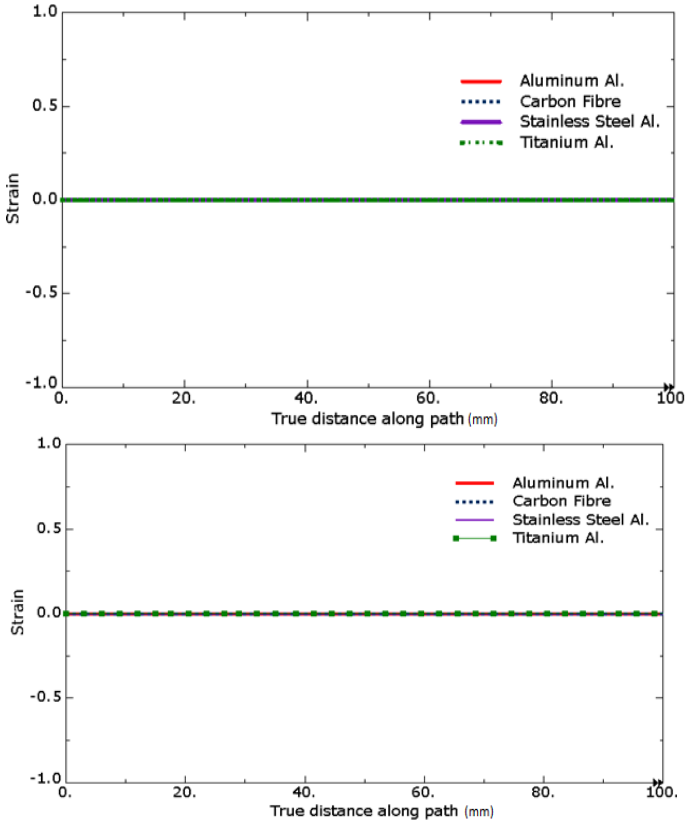

Fig. 7. Equivalent Plastic Strain (PEEQ) of the materials at the leading and trailing edges

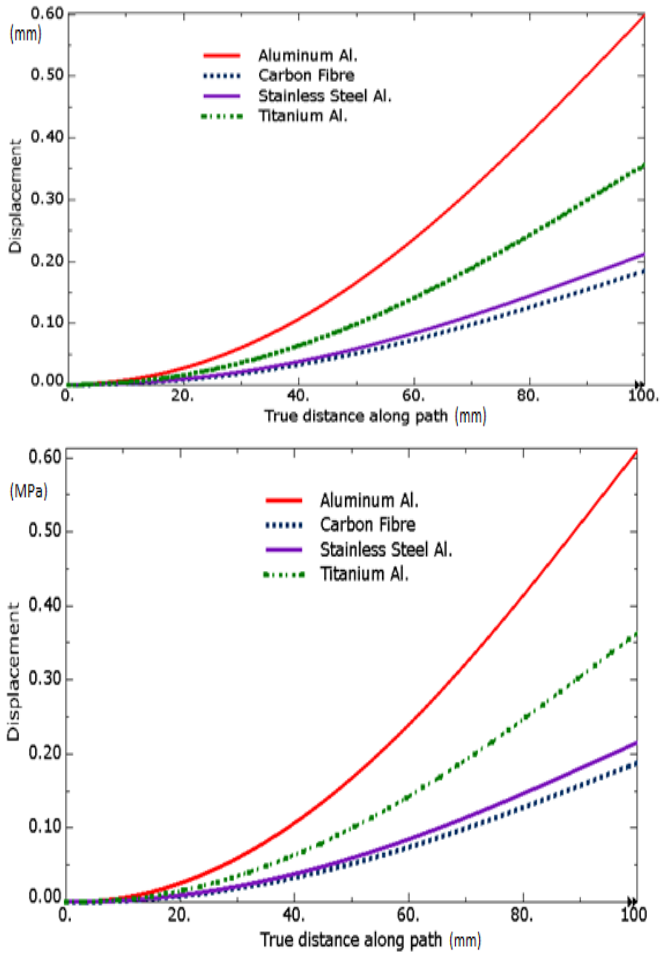

Fig. 8. The resultant displacement of the materials at the leading and trailing edges

Fig. 11 presents the stress of the materials at the central of the wing (span and root thickness respectively). The span represents the distance from one wing tip to another [17]. The results indicated that by approximation, the magnitude of stress induced in the tested materials was the same (about 19 MPa at the central span). At the central root thickness, the magnitude of stress induced was highest in stainless steel (about 20 MPa), followed by carbon fibre (about 19 MPa). The lowest stress was observed in titanium alloy (about 18 MPa), followed by aluminum whose stress values slightly exceed 18.5 MPa at the central of the wing (span and root thickness respectively). For the central span, the stresses induced were observed to decrease with increase in the true distance along the path for all the materials, but for the root thickness, the stresses induced were first observed to decrease with increase in the true distance along the path up to 2.5 mm, after which they increased with increase in the true distance along the path.

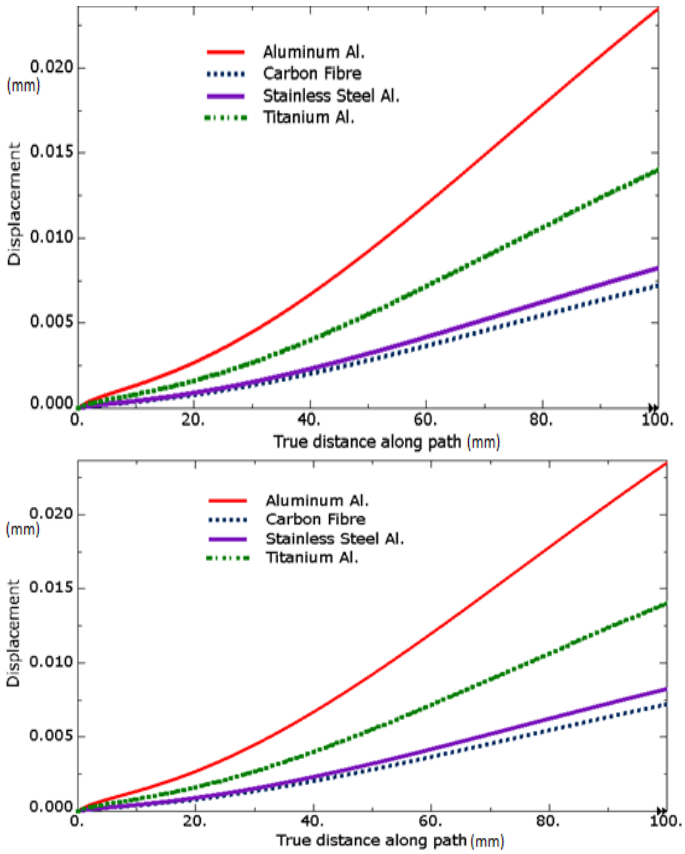

Fig. 9. Backwards displacement (U1) of the leading edge and trailing edges

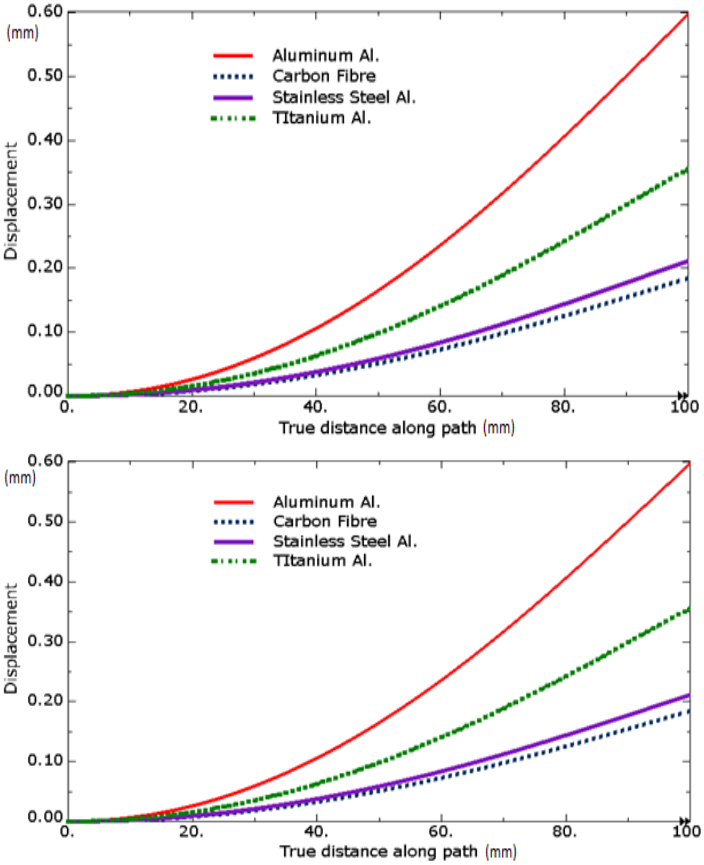

Fig. 10. Upward Displacement (U2) of the leading and trailing edges

Fig. 12 shows the maximum strain *(E_{max})* of the materials at the central of the wing (span and root thickness respectively). The results obtained indicated that the maximum strain induced in the aluminum material is the highest, exceeding 0.12 and 0.020 at the central of the wing (span and root thickness respectively). This is followed by a titanium alloy having a maximum strain value of 0.080 and 0.06 for the span and root thickness respectively. The lowest maximum strain was observed in carbon fibre whose values slightly exceed 0.03 for both span and root thickness, followed by stainless steel, whose maximum strain values slightly exceed 0.035 for both span and root thickness. For the span, initially the maximum strain was observed to increase with an increase in the true distance along the path for all the materials, after which it was observed to decrease with an increase in the true distance along the path. For the root thickness, the maximum strain induced was first observed to decrease with an increase in the true distance along the path up to 2.5 mm, after which it increases with an increase in the true distance along the path.

Fig. 13 shows that there was negligible Equivalent Plastic Strain (PEEQ) for the tested materials at the central of the wing (span and root thickness respectively). Figure 14 shows the resultant displacement (U_{mag}) of the materials at the central of the wing (span and root thickness respectively). The resultant displacement of the span was highest in aluminum (about 0.60 mm), followed by titanium alloy (0.35 mm) at the central of the wing (span). Carbon fibre has the lowest displacement (about 0.010 mm), followed by stainless steel (about 0.15 mm) at the central of the wing (span).

The resultant displacement of the span was observed to increase with increase in the true distance along the path for all the materials. The resultant displacement (U_{mag}) of the materials at the central of the wing (root thickness) is negligible (about 0).

Figs. 15 and 16 present the backward displacement (U1) and the upward displacement (U2) respectively, at the central of the wing (span and root thickness respectively). The backward displacement was highest in aluminum (exceeding 0.020 mm), followed by titanium alloy (approximately 0.0125 mm) at the central of the wing (span). Carbon fibre has the lowest displacement (about 0.005 mm), followed by stainless steel (about 0.06 mm) at the central of the wing (span). The upward displacement was highest in aluminum (exceeding 0.60 mm), followed by titanium alloy (approximately 0.35 mm) at the central of the wing (span). Carbon fibre has the lowest displacement (about 0.12 mm), followed by stainless steel (about 0.15 mm) at the central of the wing (span). Both the backward and upward displacements at the central of the wing (root thickness) are negligible (about 0). The magnitude of the upward and backward displacement at the central of the wing (span) was observed to increase with an increase in the true distance along the path for all the materials.

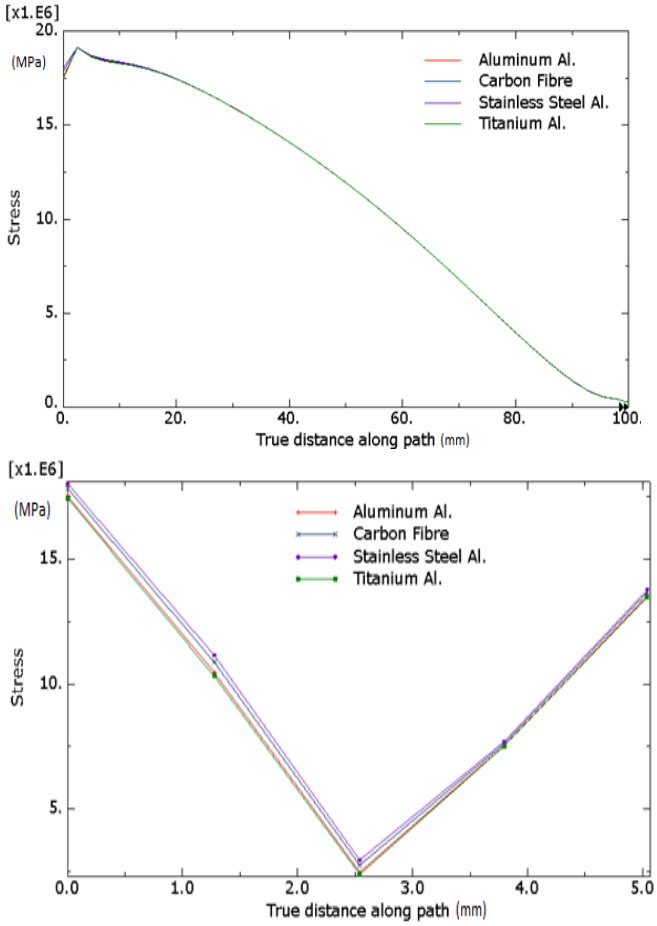

Fig. 11. Stress of the materials at the central (span and root thickness respectively)

Carbon fibre outperforms other materials with a potential for reduction in peak strain by 84% (compared to aluminium alloy under identical load), approximately 75% (compared to stainless steel under identical load) and approximately 55.6% (compared to titanium alloy under identical load). It also shows a potential for reduction in peak displacement or deformation by 83.3% (compared to aluminium alloy under identical load), approximately 57.1% compared to stainless steel under identical load, and approximately 70% (compared to titanium alloy under identical load).

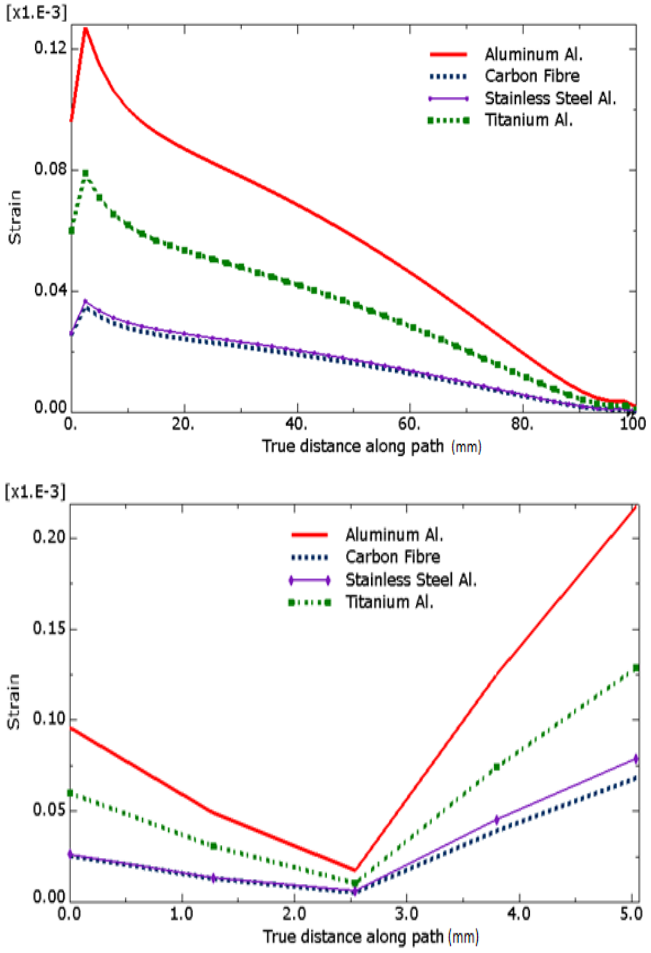

Fig. 12. Maximum strain (Emax) of the materials at the central (span and root thickness, respectively)

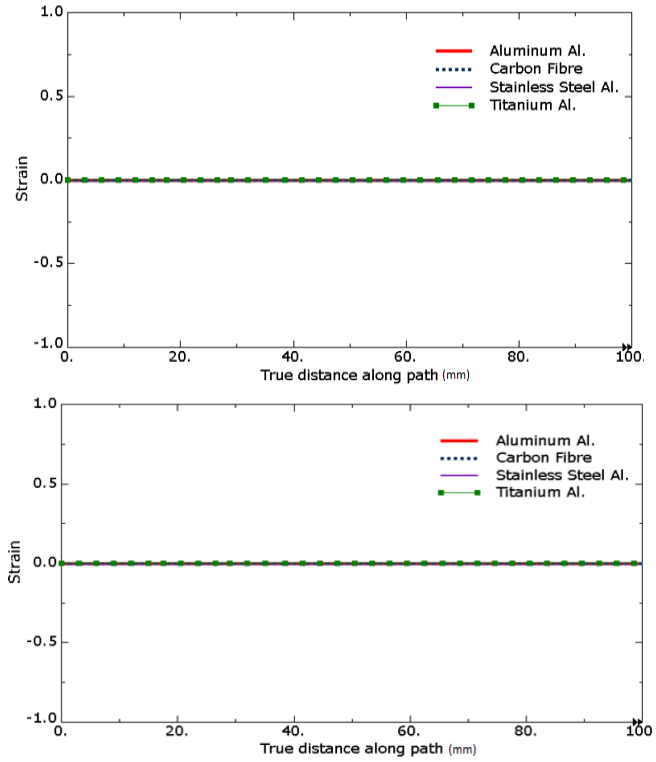

Fig. 13. Equivalent Plastic Strain (PEEQ) of the materials at the central (span and root thickness, respectively)

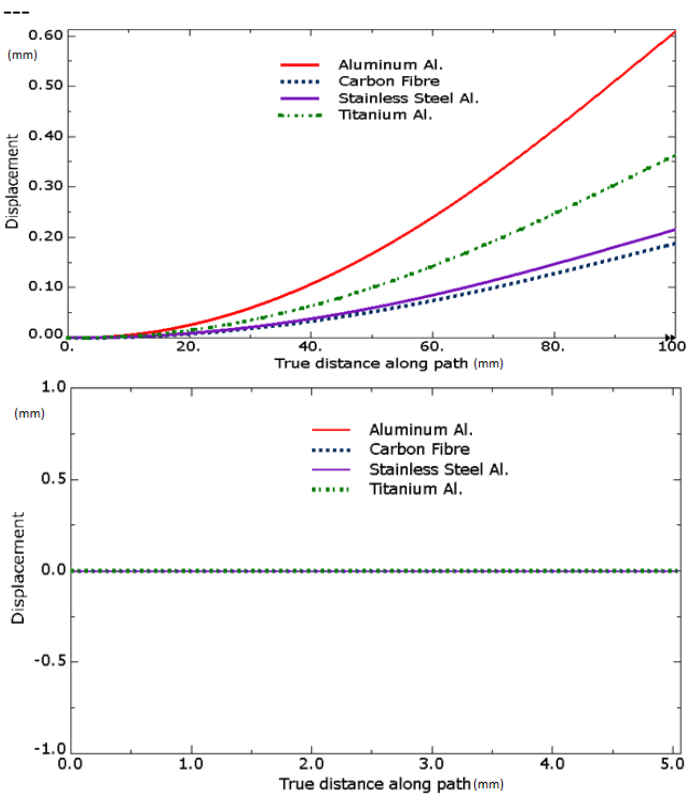

Fig. 14. Resultant Displacement (U_{mag}) of the materials at the central (span and root thickness, respectively)

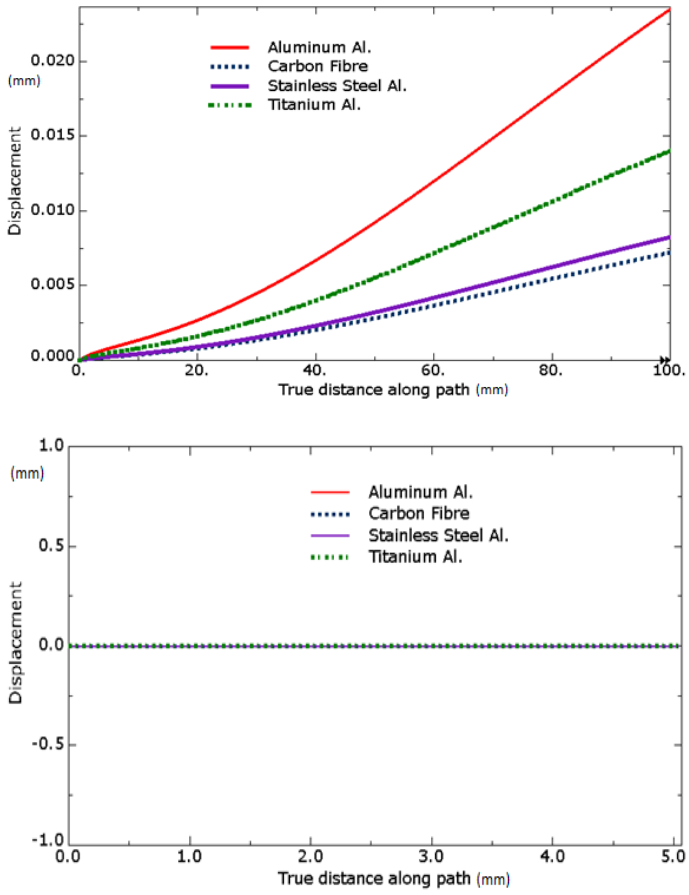

Fig. 15. Backwards Displacement (U1) of the materials at the central (span and root thickness, respectively)

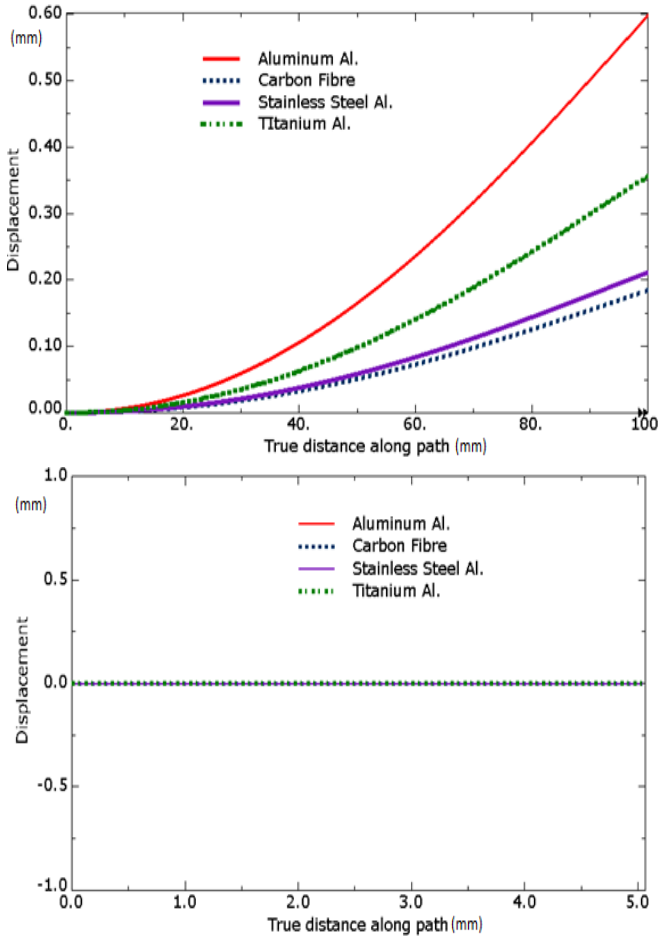

Fig. 16. Upward displacement (U2) of the materials at the central (span and root thickness respectively)

3.4 Comparison of Factor of Safety (FoS)

From the Finite Element Analysis (FEA), the maximum stress (σ_{max}) at the leading edge is 25 MPa, while that of the central (span and root thickness) is approximately 18 MPa. Therefore the average maximum stress is 21.5 MPa. Since, FEA was run at limit load, the ultimate stress becomes 1.5 × average maximum stress which gives 32.25 MPa. The yield strength of the materials are as follows: (1) aluminum alloy: 300 MPa (2) stainless steel: 250 MPa (3) titanium (Ti-6Al-4V): 880 MPa (4) Carbon fibre laminate (design allowable): 400 MPa [23,24].

Therefore, the static Factor of Safety (*FoS*) at ultimate stress is computed as follows:

1. Aluminum: $FoS = \frac{300}{32.25} = 9.30$
2. Stainless steel: $FoS = \frac{250}{32.25} = 7.75$
3. Carbon fibre (allowable): $FoS = \frac{400}{32.25} = 12.40$
4. Titanium allloy: $FoS = \frac{880}{32.25} = 27.29$

These results indicate that all the selected materials show high static *FoS* against the peak stresses obtained from the FEA simulation. This implies that the aircraft wing will not only be governed by the yield strength but by other criteria such as stiffness, deflection and buckling.

3.5 Discussion of Results

The summary of the results obtained from the computer aided modeling and simulation of the selected materials for aircraft wing application indicates that carbon fibre outperforms aluminum, titanium alloy and stainless steel in terms of the stress induced and the corresponding strain and displacement as a result of the loading conditions, for the leading and trailing edges of the wing. For the central part (root thickness), titanium alloy produced the least stress induced, followed by aluminum and carbon fibre. At the same time, stainless steel has the highest stress induced, but for the strain and displacement, carbon fibre has the best performance, followed by stainless steel and titanium alloy, while aluminum has the least performance.

Mesh convergence was achieved with an element size of 0.5 mm, which balances computational cost and accuracy. This ensures that the variations in the stresses and strains induced were negligible.

The peak stresses are nearly identical for all materials, indicating that all materials are within their elastic range and that the applied load and geometry dominate the stress distribution. Hence, their differences lie in the strain and displacement and not in the stress pattern itself. Since all materials can handle the same stress magnitude without yielding, it implies that the strength of the various materials is sufficient for the intended applications. The decisive factor becomes the stiffness (Young's modulus) and weight.

From the strain curves, aluminum alloy demonstrates the highest strain and the lowest modulus, which may indicate an undesirable or excessive flexibility under the intended application. This means that the material had the highest deformation and the lowest stiffness. The lower the strain, the higher the stiffness and vice versa. Carbon fibre composite had the least strain, highest modulus and stiffness-to-weight ratio, which implies that it can resist bending effectively. Titanium (second-highest strain) and stainless steel (moderate strain) also show relatively fairly good stiffness, but their weights might not be efficient for flight.

The displacement curves show how much the materials deform under the same applied load or aerodynamic stress. In aircraft design (especially wings), the stiffness-to-weight ratio and fatigue resistance are important criteria. The selected

material must resist bending under aerodynamic loads while maintaining a light structure.

From the displacement graphs, carbon fibre composite shows the least displacement, which implies that it has the highest stiffness. It is ideal for minimizing the wing flex and maintaining proper aerodynamic shape, leading to improved lift and lift stability. However, a reduction in displacement implies increased stiffness, which may also decrease the fatigue life of the component due to higher local stresses and a reduction in load distribution, especially under a cyclic or repeated loading condition. Next in performance is stainless steel with a moderate displacement, although it is stiff but heavy, and may reduce aircraft performance and fuel efficiency. Next is titanium alloy with a slightly higher displacement than carbon fibre and stainless steel, but less than aluminum. Aluminum performed the least with the highest displacement, which implies that it is too flexible, and may cause excessive wing deflection. The simulation results show that the concentration of the maximum stress concentrations was experienced at the leading edge. The von Mises stress observed peaked at approximately 25 MPa at the leading edge and reduced to 7.0 MPa at the trailing edge; both were found to be significantly lower than the tensile strength material (3.20 GPa), thereby indicating sufficient structural integrity. This finding is consistent with findings of Prasad et al. [25] who reported similar stress patterns during the simulation of aluminum, glass and carbon fibre for aircraft wing application using the ANSYS software. Wunderlich et al. [26] also reported improved flexibility, structural integrity and aerodynamic performance with a significant reduction in the wing mass during the optimisation of a composite aircraft wing with an increase in the aspect ratio and a reduction in the taper ratio of the wing. High stress concentration obtained at the leading edge in this study could be attributed to aerodynamic load distribution due to the fact that the leading edge directly faces the oncoming airflow, therefore, it bears the highest aerodynamic pressure. This implies that the leading edge usually carries more structural load due to its position relative to the aerodynamic centre, where there is a concentration of stresses near the front of the wing [27]. According to Bernoulli's principle and pressure coefficient distribution on airfoils, the maximum suction (negative pressure) usually occurs near the leading edge due to a steeper pressure gradient, which induces higher stress concentrations compared to the leading edge [28]. Furthermore, the curved geometry at the leading edge may trigger stress. According to stress concentration theory, areas with tight curvature usually experience high locally induced stress, compared to the trailing edge, which is thinner and may gradually dissipate stress [29].

According to Leishman [17], an aircraft wing must be designed structurally to be light-weight with sufficient stiffness to resist all the stresses and other structural load requirements. Thus, a properly designed wing will have minimal deformations under the action of the aerodynamic forces and moments. It must also resist adverse structural bending or twisting, or other aeroelastic effects.

The suitability of carbon fibre for the aircraft wing application may be traced to its high strength-to-weight ratio, high stiffness, high resistance to corrosion, fatigue, and temperature [6].

The results obtained agree significantly with the findings of Khumaedi et al. [30] that carbon fibre is a suitable material for the development of aircraft wings. However, the determination of the fiber orientation, as well as the number of fiber layers, will affect the tensile strength of the composite material and its performance for the intended aircraft wing application [31,32]. The high stress, strain and displacement induced in aluminum may be attributed to its low melting point, low fatigue strength, as well as its vulnerability to cracking and buckling under stress [4]. However, these limitations can be mitigated by mixing aluminum alloys with other metals, such as copper, zinc, magnesium, silicon, etc., to produce a higher grade of aluminum alloy with improved characteristics tailored towards aircraft wing application.

The suitability of titanium alloy for the central part of the wing (root thickness) can be linked to its high strength, high stiffness, good corrosion and fatigue resistance, as well as good durability. Its poor thermal conductivity may be responsible for the high stress, strain and displacement induced at the leading and trailing edges of the wing. However, on the titanium alloy still shows potential for aerospace component development in line with the findings of the literature [6]. The performance of stainless steel for the wing application may be impaired by its high weight. Overall, the magnitude of the stress, strain and displacement induced for the leading, trailing, and central (span and root thickness) were small. This implies the feasibility of the computer aided design and modeling of the materials vis-à-vis the intended application. Since the wings bear the entire weight of the aircraft, the wing shape is designed to be larger in its chord and thicker in cross-section near the fuselage than at the wing tips to achieve adequate structural strength and stiffness so as to

withstand large shear loads and bending moments usually produced near the root of the wing.

This work is significant in that it can assist aircraft component developers in optimising material selection for the development of aircraft wing design. Optimised designs will promote sustainability in terms of energy efficiency, light-weightiness, and environmental friendliness of the aircraft operation. Hence, the use of integrated multi-criteria decision making and simulation approach is recommended for material selection and optimisation of design during aircraft component design. However, effective process design, such as the matrix composition and processing of carbon fibre can enhance its performance for aerospace applications while the alloying of other materials, such as aluminum can improve its performance with other metals. The results obtained can assist aircraft and materials developers in their quest for the sustainability of aircraft operations.

4. CONCLUSION

The aim of this study is to employ the combination of multi-criteria decision approaches, namely RADAR-DR and RADAR-ABER, as well as computer aided modeling and simulation approach for the selection of the most suitable materials for the development of an aircraft wing.

The results obtained from the RADAR-DR and RADAR-ABER MCDM indicate that carbon fibre composite is the most suitable material for the intended application out of the other range of materials considered and stainless steel is the least preferable. Furthermore, the simulation results indicated that carbon fibre outperformed other materials in terms of the strain and displacement response to the load stress. Carbon fibre composite exhibits the lowest displacement and strain, which implies the highest stiffness with acceptable stress levels found within its elastic limits. It also has the lightest weight**,** which is crucial for fuel efficiency and payload optimization. Carbon fibre composite outperforms other materials with a potential for reduction in peak strain by 84% (compared to aluminum alloy under identical load), approximately 75% (compared to stainless steel under identical load) and approximately 55.6% (compared to titanium alloy under identical load). It also shows a potential for reduction in peak displacement or deformation by 83.3% (compared to aluminum alloy under identical load), approximately 57.1% compared to stainless steel, and approximately 70% (compared to titanium alloy under identical load).

This study bridges the computational material analysis gap via ABAQUS simulation and aerodynamic performance requirements by identifying various materials' stiffness, strength, modulus and density. These properties influence an aircraft wing's ability to bear loads and sustain lift efficiently. Carbon fibre composite was selected as the optimal material because it withstands stress (load-bearing capability), minimizes deformation (maintains lift performance) and reduces structural weight (enhances aerodynamic efficiency).

This study is significant in that it combines a scientific approach (RADAR MCDM) and a data-driven technique (ABAQUS simulation) for the selection of optimal material for aircraft wings. Thus, the outcome of this study can enhance design efficiency**,** cost reduction, and improve aircraft performance, energy efficiency and safety**.** This study also contributes to sustainable aviation via the selection of materials with the best combination of stiffness, strength, and lightweight properties.

This study is limited to material selection using RADAR-DR and RADAR-ABER MCDM approaches and the simulation of the selected materials in the ABAQUS® 2022 environment. It is also limited in the number of criteria employed and the absence of experimental validation of results. As in MCDM approaches, the determination of the weights requires some subjectivity, which may influence the prioritisation or ranking of the alternatives. However, the weighting was done in this study through expert consensus and in alignment with the literature. Future works can consider the prototyping of the aircraft wing using the empirical results obtained in this study as a guideline. Future studies can also consider a comparative analysis of the results obtained in this study using RADAR-DR and RADAR-ABER with other various MCDM, such as Analytical Hierarchy Process and Technique for Order Preference by Similarity to Ideal Solution (TOPSIS), with the incorporation of other criteria such as cost, manufacturability, and life cycle impact. Additionally, future studies can consider experimental validation of the results of this study using scaled wing prototypes or coupon testing.

CONFLICTS OF INTEREST

The author declares no conflict of interest.

REFERENCES

[1] I. Inan, I. Orhan, S. Ekici, Fuel Savings Strategies for Sustainable Aviation in Accordance with

United Nations Sustainable Development Goals (UN SDGs). *Energy,* 320, 2025: 135159. https://doi.org/10.1016/j.energy.2025.135159

[2] A. Candela, G. Sandrini, M. Gadola, D. Chindamo, P. Magri, P. Lightweighting in the automotive industry as a measure for energy efficiency: Review of the main materials and methods. *Heliyon*, 10(8), 2024: e29728. https://doi.org/10.1016/j.heliyon.2024.e29728

[3] N.F. Almussa, A. Almaktoom, The Effects of Reducing Aircraft Weight on Profitability and Fuel Consumption. *Palarch's Journal of Archaeology of Egypt/Egyptology*, 18(15), 2021: 206-214.

[4] I.A. Daniyan, F. Ale, F., Fameso, S. Mrausi, J. Ndambuki, Computer Aided Simulation and Experimental Investigation of the Machinability of Al 6065 T6 during Milling Operation. *The International Journal of Advanced Manufacturing Technology*, 133(1-2), 2021: 589–607. https://doi.org/10.1007/s00170-024-13772-9

[5] I.A. Daniyan, K. Mpofu, A.O. Adeodu, O. Adesina, Development of Carbon Fibre Reinforced Polymer Matrix Composites and Optimization of the Process Parameters for Railcar Applications. *Materials Today: Proceedings,* 38, 2020: 628-634. https://doi.org/10.1016/j.matpr.2020.03.480

[6] S.I. Sarsam, G.A.W. Majeed, Impact of Carbon Fibers on Permeable Asphalt Concrete. *Indian Journal of Engineering*, 17(48), 2020: 372-383.

[7] D.S. Vijayan, A. Sivasuriyan, P. Devarajan, A. Stefańska, L. Wodzyński, E. Koda, Carbon Fibre-Reinforced Polymer (CFRP) Composites in Civil Engineering application—A comprehensive review. *Buildings,* 13(6), 2023: 1509. https://doi.org/10.3390/buildings13061509

[8] B. Parveez, M.I. Kittur, I.A. Badruddin, S. Kamangar, M. Hussien, M.A. Umarfarooq, Scientific Advancements in Composite Materials for Aircraft Applications: A Review. *Polymers,* 14(22), 2022: 5007. https://doi.org/10.3390/polym14225007

[9] Aviation Carbon Fiber Market Size & Share Analysis - Growth Trends & Forecasts (2024 - 2029). https://www.mordorintelligence.com/industry-reports/aerospace-carbon-fiber-market (Accessed: 4 March, 2023].

[10] Aviation Carbon Fiber Market Size, Share, Competitive Landscape and Trend Analysis Report by Raw Material (PAN-based carbon fiber, Pitch-based carbon fiber), by Type (Continuous, Long, Short), by End Use (Commercial, Military, Others): Global Opportunity Analysis and Industry Forecast, 2021-2031. https://www.alliedmarketresearch.com/aviation-carbon-fiber-market-A12804 (Accessed: 4 March, 2023).

[11] D.D. Trung. A combination method for multi-criteria decision making problem in turning process. *Manufacturing reviews*, 8(26), 2021, 1-17. https://doi.org/10.1051/mfreview/2021024

[12] Toray Report, Carbon Fibre Composite Materials, https://www.cf-composites.toray/aboutus/sustainability/lci.html (Accessed: 25 October, 2021).

[13] G. Linganna**,** Carbon Fibre in Aircraft Manufacturing: Know all about it, 2023. https://www.financialexpress.com/business/defence/carbon-fibre-in-aircraft-manufacturing-know-all-about-it/3100341/#:~:text=in%20Aircraft%20Manufacturing-,Carbon%20fiber%20is%20used%20in%20a%20variety%20of%20aircraft%20components,improved%20fuel%20efficiency%20and%20performance (Accessed: 3 March, 2024).

[14] S. Kilimtzidis, A. Kotzakolios, V. Kostopoulos. Efficient Structural Optimisation of Composite Materials Aircraft Wings. *Composite Structures*, 303, 2023: 116268. https://doi.org/10.1016/j.compstruct.2022.116268

[15] S.M.O. Tavares, J.A. Ribeiro, B.A. Ribeiro, P.M. S.T. de Castro, Aircraft Structural Design and Life-Cycle Assessment Through Digital Twins. *Designs,* 8(2), 2024: 29. https://doi.org/10.3390/designs8020029

[16] S. Kumar, J-H. Seo, R. Mittal, Computational modelling and analysis of the coupled aero-structural dynamics in bat-inspired wings. *Journal of Fluid Mechanics*, 1010, 2025: A53. https://doi.org/10.1017/jfm.2025.356

[17] J.G. Leishman. Wing Shapes & Nomenclature. *Eaglepubs.erau.edu*, 31(32), 2023. https://doi.org/10.15394/eaglepub.2022.1066.n2

[18] D.D. Trung, N. Ersoy, N.T. Mai, H.X. Thinh, Applying MCDM Methods for Electric Vehicle Selection: A Comparative Study between CRADIS and PIV Methods. *Journal of Applied Engineering Science*, 23(2), 2025: 345-358. https://doi.org/10.5937/jaes0-56793

[19] N. Komatina, A novel BWM-RADAR Approach for Multi-Attribute Selection of Equipment In The Automotive Industry. *Spectrum of Mechanical Engineering and Operational Research*, 2(1), 2025: 104-120. https://doi.org/10.31181/smeor21202531

[20] N. Komatina, A Compromise-based MADM Approach for Prioritizing Failures: Integrating the RADAR Method within the FMEA Framework. *Jurnal Sistem dan Manajemen Industri*, 8(2), 2024: 72-88.

[21] J. Splichal, A. Pistek, J. Hlinka, Dynamic Tests of Composite Panels of an Aircraft Wing. *Progress in Aerospace Sciences,* 78: 2015, 50-61. https://doi.org/10.1016/j.paerosci.2015.05.005

[22] F. Fameso, D. Desai, Explicit analysis using time-dependent damping simulation of one-sided laser shock peening on martensitic steel turbine blades. *Simulation,* 96(12), 2020: 927-938. https://doi.org/10.1177/0037549720954272

[23] W.D. Callister, D.G. Rethwisch, Materials Science and Engineering: An Introduction. *John Wiley & Sons*, New York, 2020.

[24] P.K. Mallick, Fiber-Reinforced Composites: Materials, Manufacturing, and Design. *CRC Press*, Boca Raton, 2007.

[25] M. Prasad, V. K. Shankar, V. Vasu, B.Praveen, Design, Optimization and Analysis of Aircraft Composite Wing for Aerospace Application, *Tuijin Jishu/Journal of Propulsion Technology,* 44(4), 2024: 1001-4055.

[26] T.F. Wunderlich, S. Dähne, L. Reimer, A. Schuster, Global Aero-Structural Design Optimization of Composite Wings with Active Manoeuvre Load Alleviation. *CEAS Aeronaut Journal,* 13, 2022: 639–662. https://doi.org/10.1007/s13272-022-00585-3

[27] T.H.G. Megson, Aircraft Structures for Engineering Students. *Elsevier*, New York, 2012.

[28] J.D. Anderson, Fundamentals of Aerodynamics. *McGraw-Hill Education*, New York, 2011.

[29] W.D. Pilkey, D.F. Pilkey, Peterson's Stress Concentration Factors. *John Wiley & Sons*, New York, 2008.

[30] M. Khumaedi, W. Sumbodo, R. Widodo, The Tensile Strength Properties of CFRS and GRRPS for UNNES Electric Car Body Material. *AIP Conference Proceedings,* 1725(1), 020033. https://doi.org/10.1063/1.4945487

[31] I.A. Daniyan, F. Fameso, F. Ale, K. Bello, I. Tlhabadira, Modelling, Simulation and Experimental Validation of the Milling Operation of Titanium Alloy (Ti6Al4V). *The International Journal of Advanced Manufacturing Technology*, 109(7), 2020: 1853-1866. https://doi.org/10.1007/s00170-020-05714-y

[32] S.N. Phokobye, D.A. Desai, I. Tlhabadira, E.R. Sadiku, I.A. Daniyan. Comparative Analysis of the Cutting Performances of Sialon Ceramic, Cubic Boron Nitride and Carbide Cutting Tools for Titanium Machining. *The International Journal of Advanced Manufacturing Technology,* 128, 2023: 3775-3786. https://doi.org/10.1007/s00170-023-12132-3